Biofuel Droplet Evaporation Rate of a DISI Spray by Laser-induced Fluorescence and Phase Doppler Anemometry

T. Knorsch[1], L. Zigan, J. Trost, M. Wensing, A. Leipertz
Dept. Engineering Thermodynamics (LTT) and Graduate School in Advanced Optical Technologies (SAOT), FAU Erlangen-Nuremberg, Germany
Tobias.Knorsch@ltt.uni-erlangen.de and Lars.Zigan@cbi.uni-erlangen.de

Abstract

The atomization and evaporation of gasoline sprays with bio-components differs depending on the respective alternative fuel blend physiochemical properties. This work focuses on estimating the biofuel evaporation rate of sprays at stratified charge conditions. One specific spray plume is analyzed in terms of local droplet size verified by local vapor concentration and temperature. Depending on the operating conditions different physiochemical properties were found to dominate the atomization and evaporation behavior. For moderate ambient temperature and pressure high-boiling point components show a strong influence on the droplet size and temperature distribution in the sprays. However, at elevated temperature the evaporation rate changes completely. Due to a high degree of evaporation taking place, cold spots of 125 K temperature difference appear inside the spray and during the spray process. In the center of the spray plume a maximum cooling of 89 K due to the higher droplet density in those areas compared to the more dilute outer positions are detected. However, when comparing data of two diffident boundary conditions with an ambient temperature difference of 200 K, the measurement positions in the outer regions of a spray cone always show higher temperatures. Smaller droplets as a measure of progressed evaporation are found there. For fuel mixtures with higher evaporation enthalpy the temperature difference between spray center and spray boundary is more pronounced than for fuels with a lower evaporation enthalpy – despite their higher boiling point. Overall, it can be stated that for the droplet evaporation at stratified supercharged conditions, the evaporation enthalpy is a dominating physiochemical property.

Introduction

Due to downsizing and high supercharging of internal combustion (IC) engines the thermal load of engines is increased. Higher compression temperatures of charged direct-injection spark-ignition (DISI) engines have an influence on the complete combustion reaction chain. The process chain also depends on the evaporation enthalpy of the respective fuel, whereas the fuel variety is expanding already due to the addition of biofuel or synthetic fuels to fossil fuels. In a context where the biogenic component of gasoline blends is demanded to increase by law over the coming years, there is a need to understand the atomization and evaporation mechanisms of both gasoline and of these alternative fuels to optimize fuel efficiency and minimize the production of harmful emissions. This requires a detailed analysis of the processes which dissolve fuels within some milliseconds into hundred thousands of droplets and simultaneously change their temperature by some hundred Kelvin.

The complexity of the spray processes of ordinary gasoline fuels is often simplified by using single-component surrogate fuels. However, those pure fuels like isooctane or n-heptane are not capable to model realistic gasoline spray behavior [1]. Currently, this is of special interest considering blends with biogenic fuels such as ethanol, n-butanol and isobutanol, which show significant differences in physiochemical properties changing the atomization and evaporation behavior. For fuel stratification conditions or injection during catalysator heating with late injection timing an inhomogeneous temperature distribution throughout the cylinder and the spray occurs. This determines local inhomogeneities in the evaporation rates and, therefore, mixture formation and ignitability. Spatially-resolved information of the temperature and droplet size during and after injection is required to locally determine the evaporation rate and evaporation cooling in the spray as well as the affinity to pre-ignition or soot formation. In general the spray plumes of DISI injectors cool down the surrounding gas whereby the spray cone centers are typically expected to show lower temperatures due to the higher droplet density whereas in outer regions the concentration is lower due to stronger air entrainment. The spatial distribution of this cooling depends on the specific initial fuel temperature, the fuel amount per injection, pressure, evaporation enthalpy, and local concentrations. In this work the droplet sizes and absolute temperatures are measured at some selected positions and boundary conditions to assess fuel dependent evaporation.

Spray measurements are carried out using an optically accessible high temperature / high pressure spray chamber and applying a setup with 0-D/2-D optical measurement techniques. First, planar Mie scattering meas-

[1] Corresponding author: Tobias.Knorsch@ltt.uni-erlangen.de

urements of the liquid phase using gasoline E10 are carried out to analyze the liquid spray distribution and determine relevant 0-D positions for the phase Doppler anemometry (PDA) measurements. In addition, a study using two-line planar laser-induced fluorescence (2line-PLIF) is carried out. In this way, a distribution of the droplet size and local temperature after the injection end can be calculated. This information is required to locally estimate the evaporation rate and cooling inside the spray plumes. For the PDA measurements, different 0-D positions through one specific spray plume are analyzed to give information about droplet size and velocity for estimating the droplet evaporation rate, which is compared with the results of the PLIF measurements.

Planar laser-induced fluorescence (PLIF) based on fuel tracers is commonly used to characterize the mixture formation for engine combustion or technical combustion processes [2] and is capable to determine the temperature distribution in the gas phase. Up to now, there are very few measurements with optical techniques to determine the temperature fields in sprays at engine conditions. The studies of Rothamer et al. [3], Luong et al. [4], Devillers et al. [5] already showed the potential of the two-line excitation LIF measurement technique regarding the accuracy and single-shot precision under engine conditions without injection. Tea [6] showed in a proof-of-principle study the application of 2-color LIF to measure the vapor temperature at diesel injection conditions. Due to the temperature dependency of the fluorescence signal, simultaneous measurements of fuel vapor concentration and temperature are possible. For thermometry, the tracer 3-pentanone, which already presented a high suitability in other works [3,7], is applied. However, the evaporation of multi-component fuels (such as fuel-tracer mixtures) can show demixing of fuel components in the droplet under DISI conditions with injection in high-pressure atmosphere [1,8-9]. It was also reported that mixtures of 3-pentanone and isooctane behave in a non-ideal manner [10] even though the normal boiling points of the components are well matched. Thus, the evaporation rates of the components may be different. However, the mixing process inside a droplet in a turbulent flow may show different results and lead to varied conclusions as reviewed by Schulz and Sick [2].

A combination of both optical techniques is used to determine interferences of both the evaporation rate and the direct impact on the respective droplet sizes for different biofuel mixtures. To use the measured temperature field by PLIF and droplet sizes achieved by PDA to assess the evaporation and mixing is rather challenging due to the time-shifted information.

Experimental Methods

In this study for both the atomization and evaporation measurements isooctane as a widely applied standard reference fuel is examined and compared with two 3-component biofuel mixtures (high and low RON) as well as the pure biofuels n-butanol and ethanol. The 3-component fuel with RON46 ‘3K’ contains a low, middle and high-point component and thus matches the boiling curve of gasoline (figure 1) [1,11] and was proved to model the multicomponent fuel atomization and evaporation of gasoline [1]. The other 3-component fuel ‘3ZK’ with RON95 was especially designed to study the role of evaporation enthalpy for spray evaporation and ignition phenomena in the future. However, the boiling curve of gasoline is also approximated by ‘3ZK’ (figure 1, table 1). The multi-component evaporation is a highly non-steady-state process and probably a demixing of the fuel components in the droplets occurs. Therefore, the composition is chosen according to the boiling point diagram to cover the main fuel components for a more realistic spray behavior compared to single component fuels (table 1). As a tracer for the laser-induced fluorescence measurements 3-pentanone (20% vol.) is added to non-fluorescent surrogate fuel mixtures. Gasoline itself partially consists of aromatic fuel components which may vary depending on the vendor. Thus, its vapor phase might be hard to quantify and just its liquid phase was investigated within this work.

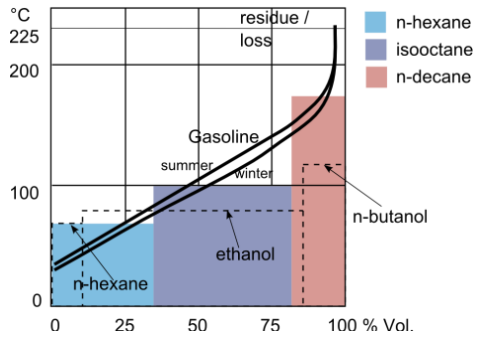

Figure 1 Boiling point diagram of gasoline [12] with indicated boiling points of the fuel components for ‘3K’ (colored blocks) and ‘3ZK’ (dashed).

Table 2 presents the applied modern DISI boundary conditions to compare the effects of boiling point and evaporation enthalpy for different engine loads. Table 3 presents the investigated fuels with their physiochemical properties and specific values at ambient boundary conditions. The kinematic viscosity is more relevant for cold

boundary conditions which previous measurements could demonstrate [1,11]. The RON (research octane number) will become important for ignition measurements in a subsequent work.

Table 1 Composition of fuel mixtures '3K' and '3ZK'.

fuel component	**'3K'** % vol.	**'3ZK'** % vol.
n-hexane	25	10
isooctane	45	-
n-decane	20	-
ethanol	-	75
n-butanol	-	15

Table 2 Applied chamber boundary conditions for both liquid and vapor phase investigations.

OP	**p_{Gas} / MPa**	**T_{Gas}/K**	**p_{Fuel}/MPa**	**T_{Fuel}/K**	**$t_{inj.}$/ ms**
#1	0.56	473	20	353	1
#2	0.80	473	20	353	1
#3	0.80	673	20	353	1

Table 3 Investigated fuel mixtures and fuel components with key physiochemical parameters at ambient conditions (20°C / 1 bar) [13-15], bold = besides PDA also investigated with PLIF.

fuel	**boiling point / °C**	**RON / -**	**kin. viscosity / 10^{-6}m²/s**	**evap. enthalpy / kJ/kg**	**density / g/cm³**
isooctane	99	100	2.95	305.4	0.70
n-butanol	118	96	3.74	637.7	0.80
ethanol	78	109	1.22	938.2	0.80
3K	69-174	~46	-	334.7	0.67
3ZK	69-118	~95	-	844.6	0.79
gasoline E10	~46-207	95	~0.57	~350	~0.76
n-hexane	69	19	0.46	363.6	0.66
n-decane	174	-41	1.9	352.5	0.72
3-pentanone	(=tracer) 102	-	0.62	440.7	0.73

In order to achieve precise measurement data, reproducible conditions have to be set up. Therefore, an optically accessible high temperature / high pressure spray chamber was used for all measurements. This combustion test rig was designed for spray investigations at conditions up to boundary conditions of 1000 K and 10 MPa. The investigated 6-hole injector (Bosch HDEV 5.2) has a geometric spray angle of 55°; the bent angle is 10°. The fuel and the injector are conditioned to 353 K similar to engine wall temperatures and the injection duration is set to 1 ms, which results in an injected mass of 12.4 mg/pulse at 20 MPa injection pressure. The radial liquid distribution was achieved by Mie scattering using a frequency-doubled Nd:YAG laser (Quantel Brilliant B) which are recorded on two different measuring planes (figure 2).

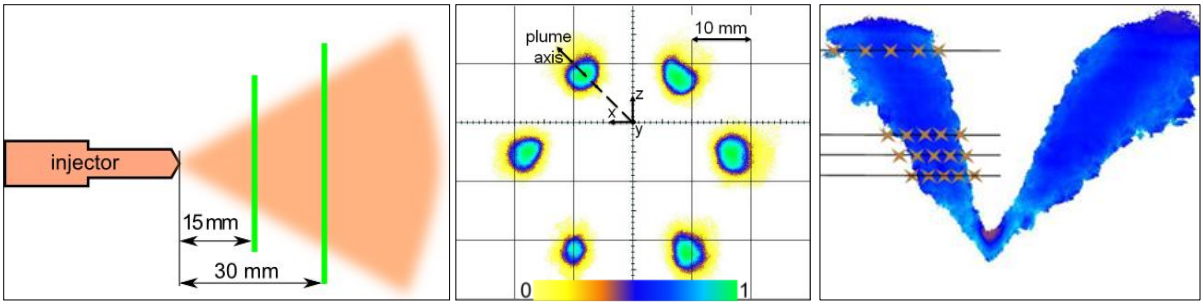

Figure 2 Schematic of the radial Mie measuring planes (left), Mie scattering mean image in combination with plume axis for PDA measurements (middle) and spatially-resolved spray vapor temperature distribution of the LIF study (right).

The measurement planes for both droplet size and temperature are set to 15 mm and 30 mm from the nozzle tip for estimating the droplet evaporation rate. These planes correspond to the area of secondary breakup, small Weber numbers are expected. The droplet sizes and velocities are measured by a commercial PDA system (Dantec HiDense BSA P80), which is mounted on a three-axial traverse (figure 3). In this manner, the laser emitter can be moved simultaneously and precisely with the signal receiver to any desired measurement location within the spray chamber. A Coherent Innova 300 argon ion laser is used offering a maximum power of 9W (488 nm and 514.5 nm). The beam spacing is 60 mm and the emitter lens has a focal length of 310 mm, thus the resulting quasi 0-D elliptical PDA measurement volume is 761 µm in width by 74 µm in height. Both measure-

ment planes include five measuring points from the spray cone center to the outermost regions of the respective spray plume (figure 2, right).

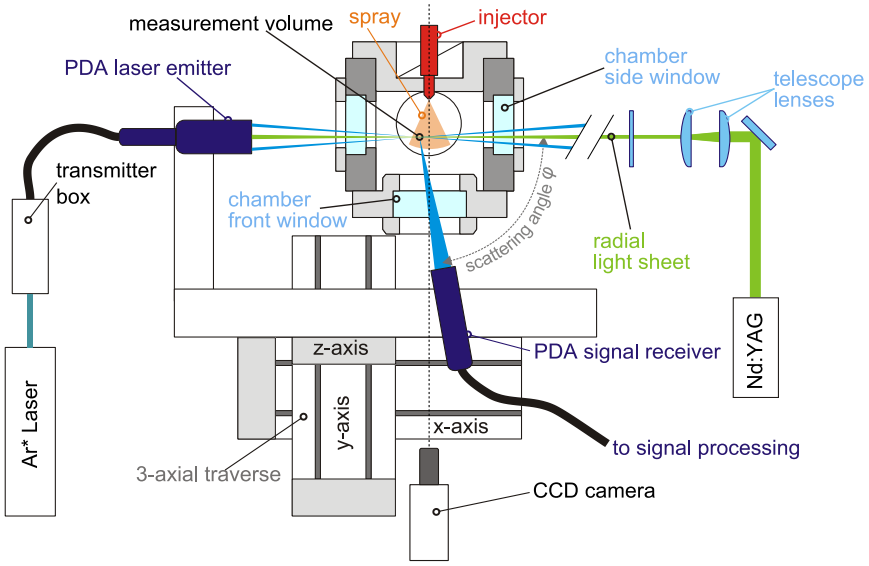

Figure 3 Optical spray chamber with PDA system on a traverse in combination with one-way Nd:YAG laser excitation for definition of PDA measurement positions.

Spatially-resolved droplet size distribution and related temperature are presented to estimate the atomization and evaporation. The focus of this work is the evaporation, thus the droplet velocity is neglected as we measured non-coincident in order to achieve high droplet size signal gain. To measure the temperature and concentration distribution under engine-relevant conditions laser-induced fluorescence is applied. The fuel spray is excited by two different excimer lasers (248 nm KrF, 'Radiant Dyes EXC-400' / 308 nm XeCl, 'Lambda Physik LPX110'). The fluorescence signals were recorded by a double-shutter ICCD camera; vapor temperature distribution is calculated from the signal intensity ratio S308/S248 which has been calibrated depending on temperature, pressure and mixture composition in a flow cell in advance. Mixture fraction of the fuel is calculated from 248 nm fluorescence and the known temperature field. The average temperatures show a systematic error of 3.8%; more details can be found in reference [16]. The chamber pressure and temperature are set to three different operating points (table 2), respectively, to model late injection timing. The chamber is scavenged continuously with nitrogen to remove the fuel between injections. The gasoline surrogate fuels contain 20% 3-pentanone (by volume) as fluorescence tracer. The optical PLIF setup is the same which was used for the required tracer calibration measurements in advance.

Spatial fluctuations of the beam profile are reduced by a beam homogenizer, after which the beam has a height of about 20 mm and is slightly diverging [17]. Afterwards, a thin light sheet is formed with cylindrical plano-convex lenses. The two beams are overlapped with a dichroic mirror. The height of the light sheet is 50 mm for the spray measurement. For the correction of laser intensity fluctuations the reflection of a fused silica glass plate is measured with an energy meter. The beam is then directed through the cell and absorbed totally in a beam dump. The fluorescence signal is collected perpendicular to the laser light sheet. A 355 nm longpass filter is used to block elastically scattered light from the lasers. The signal is recorded with an ICCD camera with an exposure time of 240 ns to avoid the detection of the longer lasting phosphorescence that occurs for lower oxygen partial pressures [18]. A PCO 'dicam pro' with double-shutter mode and no binning is used, the time delay between the respective two recorded images is set to 5 µs. The raw data are evaluated in a way that the very same positions of the PDA droplet size measurements are matched. The evaluated averaged PLIF area was 900 µm x 300 µm for each PDA spot.

Results and Discussion

In this paper the influence of ambient pressure and temperature difference on the spray behavior in terms of atomization and evaporation for different fuel and biofuel mixtures is investigated. For the droplet sizes measured by PDA, five different measurement positions through one specific spray plume give information about the droplet size from the spray outer region, spray plume center and spray intermediate region. Figure 4 shows droplet distributions in a histogram (average of 5 measurement positions through one plume) as well as arithmetically averaged droplet size for some exemplary fuels in two planes of the spray plume for OP#3.

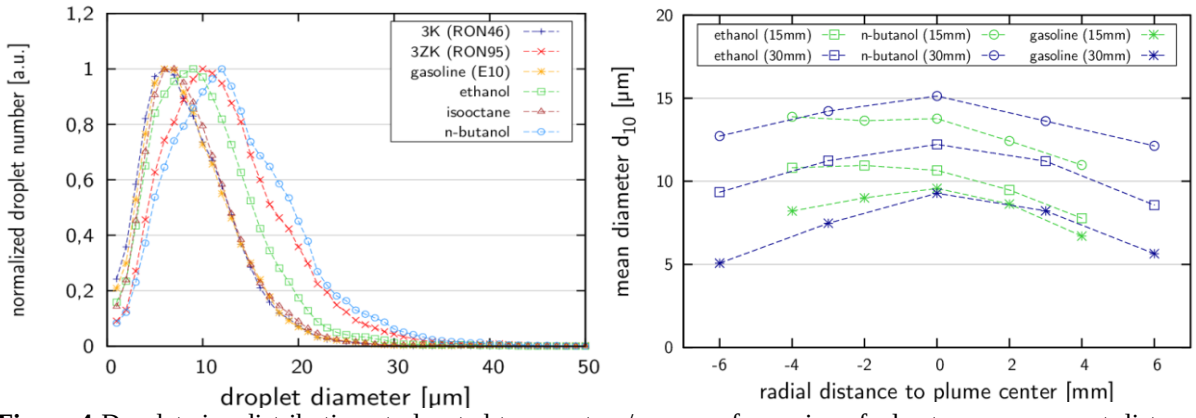

Figure 4 Droplet size distribution at elevated temperature/pressure for various fuels at a measurement distance of 15 mm from the nozzle tip (left) and spatially-resolved droplet diameter through one spray plume for two measurement planes from the nozzle tip (15 and 30 mm) (right) for OP#3 (0.8MPa, 673 K).

N-butanol as a higher viscosity fuel with the highest boiling point of the investigated fuels and a relatively high evaporation enthalpy shows the largest droplet mean diameters (figure 4, left) for both measurement planes (15 mm / 30 mm). During the measurements we also observed the lowest droplet velocities for this fuel. However, as we focus on the droplet size the measurements are examined non-coincident, the droplet velocity is excluded. The 3-component '3K' fuel with RON46 matches the droplet size distribution of gasoline as it contains a low, middle and high-boiling point component [1]. This proves the similar atomization and evaporation behavior for '3K' and gasoline, which was also demonstrated for another injector at different conditions (1.5 MPa, 473 K), see Ref. [1, 11]. Isooctane worked well as a surrogate fuel for gasoline for this specific operating point. '3ZK', however, behaves more like a high-boiling point fuel, as it consists only of 10% vol. n-hexane thus it shows droplet sizes closer to those of n-butanol. Despite its large amount of ethanol, the droplet sizes of '3ZK' are larger than for the pure ethanol fuel. This confirms the large effect of the high-boiling point fuel components despite their low fraction in the mixtures [1]. Ethanol shows droplet sizes much larger than gasoline due to its high evaporation enthalpy, which limits the evaporation rate after a certain time. For OP#1 and OP#2 this trend is less pronounced. The higher the gas temperature is, the larger the droplet size difference of ethanol to gasoline and isooctane occurs, see figure 5 and 6. The main result in the spatial size distribution (figure 4, right) is that the largest droplet diameters are present for n-butanol over the complete plume cross-section for both measuring planes. In general, the droplet sizes are larger for further distances as collision effects may take place and very small droplets may evaporate before reaching the 30 mm distance.

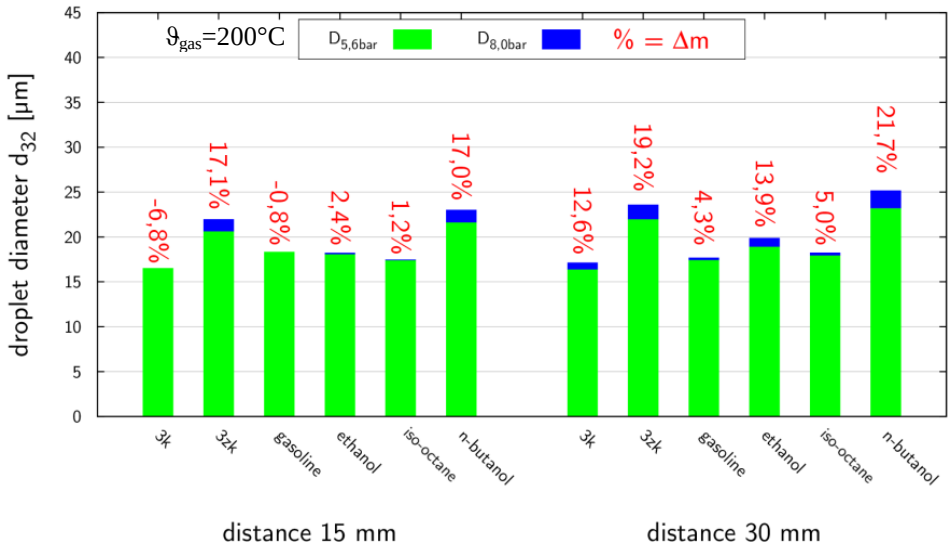

Figure 5 Droplet sizes (d_{32}) for two different gas pressures OP#1 (5.6 bar) vs. OP#2 (8 bar) for constant gas temperature = 200°C; Δm = relative mass difference based on arithmetically averaged droplet size.

To clearly present the fuel dependent change in droplet size, arithmetic mean diameter bar graphs for all investigated fuels are presented in figure 5 and 6. The respective PDA measurement position of the spray plume center (figure 2) for both measurement planes was validated in order to include only ballistic propagating drop-

lets. Investigations at moderate pressure conditions OP#1 (5.6 bar) show an increasing influence of the evaporation enthalpy compared to previous tests [19], which showed that at low pressure ethanol behaves like a low-boiling point component; the evaporation enthalpy influence seemed to be minor. In this previous work, the droplet sizes of ethanol at low pressure were approximately 20% smaller than those of isooctane. However, in this transition region (OP#2) they are greater due to the high evaporation enthalpy becoming more important. While for the measurement plane of 15 mm the droplet size difference of 1 µm between isooctane and ethanol is not that significant, more-distant at 30 mm to the nozzle tip the evaporation enthalpy of ethanol limits the evaporation rate (figure 5) while isooctane shows 3 µm smaller droplets. Figure 5 also shows that in addition to n-butanol ethanol behaves more like a high-boiling point component and shows larger droplets despite of the relatively low boiling point. N-butanol shows the highest difference in droplet mass as the boiling point is 174°C at 5.6 bar and 191°C at 8.0 bar, which is close to the gas temperature (200°C). Thus, for OP#2 n-butanol shows lower evaporation rate compared to OP#1. This effect can also be seen for '3ZK' due to its small amount of n-butanol. The evaporation behavior for these boundary conditions is more influenced by the boiling point than by the evaporation enthalpy.

At increased ambient pressure conditions (8 bar, 400°C) the main influences change significantly. The evaporation behavior of ethanol is now closer to that of the high-boiling point n-butanol (figure 6), which implies that the influence of the evaporation enthalpy increases. For the low volatility isooctane the increase of 200 K ($D_{200°C}$ vs. $D_{400°C}$) causes a reduction in the arithmetic drop mass by 63.9%. However, the mass of ethanol drops in this hot environment decreases only 47.1% due to its high evaporation enthalpy. Basically, the strong influence of the high-boiling point n-butanol in the 3-component fuel '3ZK' is observed – even though only 15 vol. % of it is contained in '3ZK'. Its main component ethanol has less effect on the evaporation on the 30 mm measuring plane where the momentum exchange with the ambient gas is almost completed. Even those low amounts of high-boiling point components show a great influence on the droplet evaporation for all operating points. In low pressure measurements the boiling point is found to be the main influencing thermophysical property [19]. For moderate pressure conditions at elevated temperature the influences of the properties boiling point and evaporation enthalpy counteract to this behavior (OP#2). At very high gas pressure and temperature conditions (OP#3), the evaporation is strongly dominated by the evaporation enthalpy as proved simply by comparing the fuels '3ZK', ethanol and n-butanol.

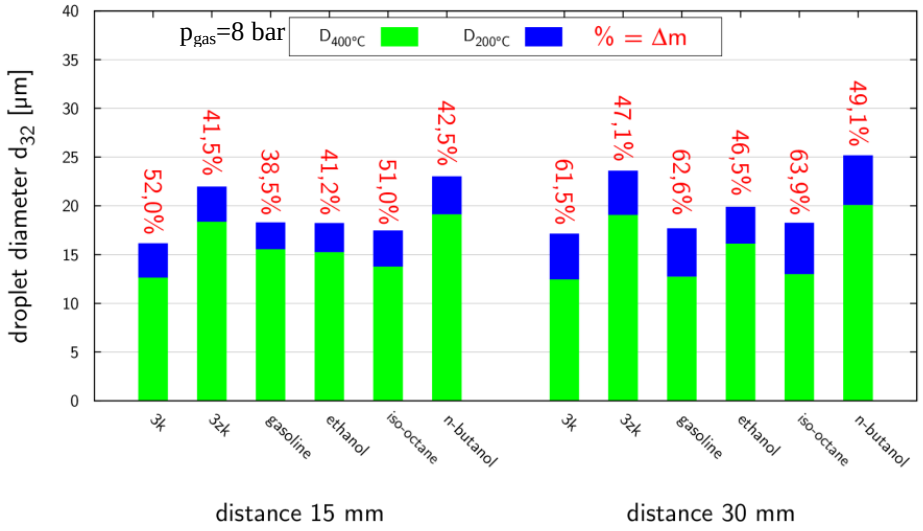

Figure 6 Absolute droplet sizes for two different gas temperatures (OP#3 400°C vs. OP#2 200°C at an ambient pressure of 8 bar); Δm = arithmetic change in droplet mass (temperature difference of 200 K).

The phenomena of fuel dependent evaporation rate described so far are also detectable in the PLIF measurements in terms of observed vapor temperature and concentration. However, those temperatures are recorded in between 2 ms and 4 ms after visible start of injection, and thus after the PDA measurement time (0-2 ms after start of injection). However, this combination is robust enough to underline the phenomena studied with the help of droplet size data. The absolute temperature values are verified by a CFD model using a transient RANS approach including all relevant submodels for a realistic spray representation, details are in reference [16]. In general the spray plumes cool down the mixing layer between vapor and surrounding gas (figure 7) for all three boundary condition sets. As expected the spray cone centers show lower temperatures due to the higher droplet concentrations in those areas, whereas in outer regions the vapor concentration is lower (figure 8).

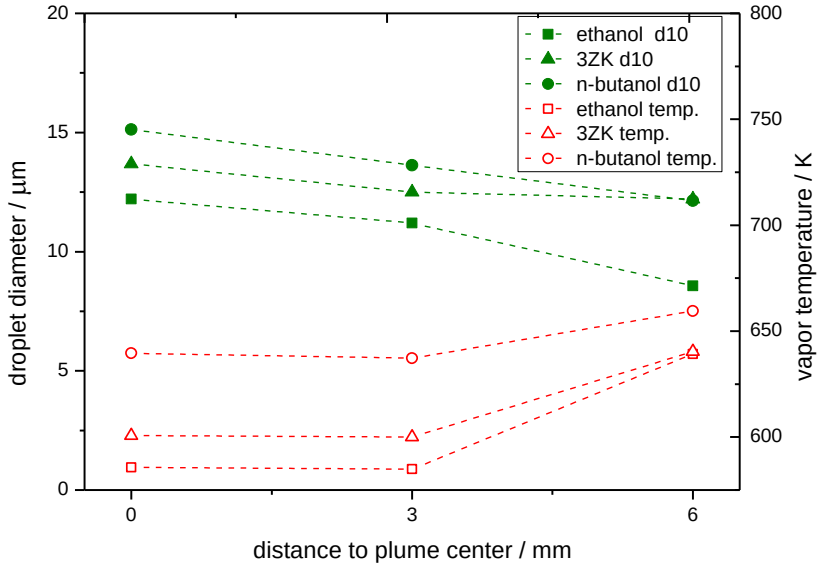

Figure 7 Absolute droplet sizes and spray vapor temperatures, OP#3 (0.8MPa, 673K)

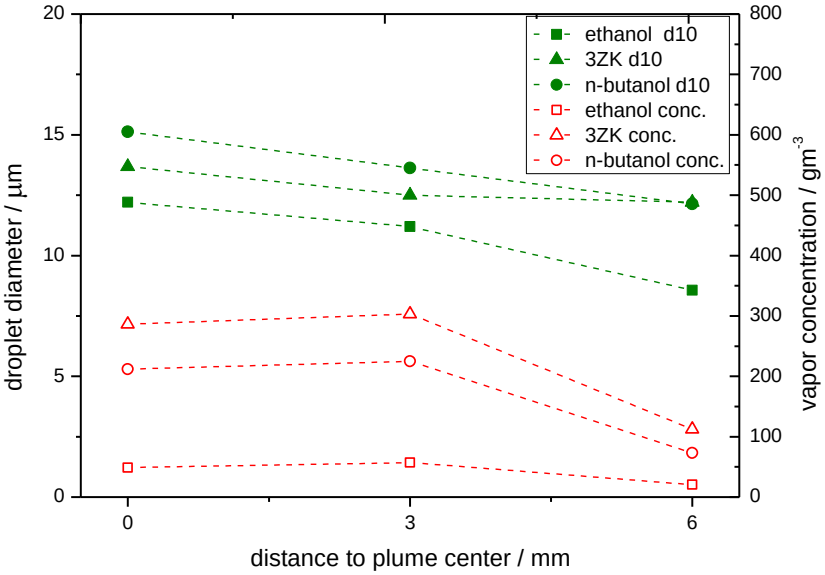

Figure 8 Absolute droplet sizes and spray vapor concentrations, OP#3 (0.8MPa, 673K)

Within this work data of two diffident boundary conditions with either a temperature or a pressure difference are compared. The measurement positions of the plume outer regions show smaller droplets as a measure of progressed evaporation and air entrainment. These regions always show higher temperatures due to stronger fuel-air mixing. Positions in the spray, which present a low vapor concentration, always show smaller local evaporation cooling and lower droplet sizes for all investigated fuel mixtures. However, fuel mixtures with a higher evaporation enthalpy cool down the mixture more than fuels with a low evaporation enthalpy – even if they have a higher boiling point, i.e. slower evaporation rate and therefore different spray shape. The trend of the fuel-dependent droplet sizes matches the ratios of the temperature decrease, which follows the fuel evaporation enthalpy. This can be seen for instance for n-butanol with an evaporation enthalpy of 637.7 kJ/kg compared to ethanol with 938.2 kJ/kg in figure 7. The maximum cooling is 36 K for n-butanol, 73 K for '3ZK' and 89 K for ethanol. This trend corresponds to the evaporation enthalpy values (table 3).

Summary and Conclusions

In this study a variety of single component fuels and mixtures are tested at different ambient conditions to identify most significant fuel properties and their effects on the atomization and evaporation. The gained local temperatures as a function of spray impulse, mixture of vapor with entrained gas as well as the chemical data of evaporation enthalpy and boiling point confirm the results of the droplet size measurements. In various investigated engine conditions different physiochemical properties dominate the evaporation rate. For moderate ambi-

ent conditions such as 0.56 MPa / 473 K isooctane, gasoline and ethanol and '3K' show similar evaporation rates by similar droplet sizes, despite large differences in the chemical data of boiling point, vapor pressure and evaporation enthalpy of the single component fuel. N-butanol as a very high-boiling point fuel with relatively high evaporation enthalpy lead to the largest droplets for this operating point, followed by '3ZK' (RON95). Even though the 3-component mixture '3ZK' contains only 15% by volume of n-butanol, the behavior appeared more similar to n-butanol than to ethanol, which is 75% of the '3ZK'. Thus, the high-boiling point components show a very strong effect on the spray behavior and droplet distribution.

At elevated gas pressure and temperature (0.8 MPa / 673 K) the evaporation rate changes completely. Due to a high degree of evaporation taking place, the studied fuels present a stronger difference in droplet size and surrounding temperature after evaporation. Isooctane with a higher boiling point than ethanol show much smaller droplets than ethanol. Due to the very high evaporation enthalpy of ethanol, the droplet evaporation rate is limited. Thus, ethanol behaves much more like a high-boiling point fuel such as n-butanol. The phenomenon of '3ZK' mentioned above remains, the component n-butanol with 15% by volume in the mixture delivers droplets similar to n-butanol rather than to the main component ethanol. However, the evaporation cooling of ethanol is maximal due to the high evaporation enthalpy. The trend of the droplet sizes matches the trend of the temperature decrease, which follows the evaporation enthalpy ratios. This can be seen for n-butanol with an evaporation enthalpy of 637.7 kJ/kg compared to ethanol with 938.2 kJ/kg. The mean cooling along the three measurement points is 36 K for n-butanol, 73 K for '3ZK' and 89 K for ethanol. This trend corresponds to the evaporation enthalpy values. Thus, it can be stated that for stratified charge conditions with high pressure and temperature, the evaporation enthalpy is the dominating physiochemical property for the evaporation rate. The knowledge of the evaporation rate in dense sprays can be used for further model development and validation as well as to accelerate the optimization of injection and combustion strategies for modern fuels and blends.

Acknowledgements

The authors gratefully acknowledge the financial support for parts of this work from the Erlangen Graduate School in Advanced Optical Technologies (SAOT) within the framework of the German Excellence Initiative by the German Research Foundation (DFG). Furthermore, this work and setup was supported by the Bavarian Research Foundation (BFS) in the framework of the project 'AZ-932-10: WiDiKO'. We also like to thank Dr. Bodo Durst (BMW Group Munich, CAE Combustion) and Prof. Dr. Christian Hasse (TU Freiberg, NTFD) for the technical support and cooperation within this project.

References

[1] Zigan, L., Schmitz, I., Flügel, A., Knorsch, T., Wensing, M., and Leipertz, A., *Energy Fuels* 24: 4341-4350 (2010)
[2] Schulz, C., and Sick, V., *Prog. Energy Combust. Science* 31-1: 76-121 (2005)
[3] Rothamer, D.A., Snyder, J.A., Hanson, R.K., and Steeper, R.R., *Appl. Physics B* 99: 371-384 (2010)
[4] Luong, M., Zhang, R., Schulz, C., and Sick, V., *Appl. Physics B* 91: 669-675 (2008)
[5] Devillers, R., Bruneaux, G., and Schulz, C., *Appl. Physics B* 96: 735-739 (2009)
[6] Tea, G., Bruenaux, G., Kashdan, J.T., and Schulz, C., *Proc. Combust. Institute* 33-1: 783-790 (2011)
[7] Einecke, S., Schulz, C., and Sick, V., *Appl. Physics B* 71-5: 717-724 (2000)
[8] Makino, A., and Law, C.K., *Combust. Flame* 73-3: 331-336 (1988)
[9] Zigan, L., Ammon, M., Gupta, A., Wensing, M., and Leipertz, A., *SAE Int. J. Fuels Lubr.* 5-1: 254-264 (2012)
[10] Davy, M., Williams, P., Han, D., and Steeper, R., *Exp. Fluids* 35-1: 92-99 (2003)
[11] Zigan, L., Schmitz, I., Flügel, A., Wensing, M., and Leipertz, A., *Fuel* 90: 348-363 (2011)
[12] Pischinger, S. Verbrennungsmotoren, Band I, 21st edition, RWTH Aachen, 2000
[13] Institut für Arbeitsschutz der Deutschen Gesetzlichen Unfallversicherung: *GESTIS-Stoffdatenbank*. website: http://gestis.itrust.de, pageview 12/11/2011
[14] Bronkhorst High-Tech B.V.: FLUIDAT on the web. website: http://www.fluidat.com, pageview 12/19/2011
[15] Eyidogan, M., Ozsezen, A.N., Canakci, M., and Turkcan, A., *Fuel* 89: 2713-2720 (2010)
[16] Trost, J., Zigan, L., and Leipertz, A., *12th Triennial Int. Conference on Liquid Atomization and Spray Systems*, Heidelberg, Germany, September 2 - 6, 2012
[17] Pfadler, S., Beyrau, F., Löffler, M., and Leipertz, A., *Optics Express* 14-22: 10171-10180 (2006)
[18] Löffler, M., Beyrau, F., and Leipertz, A., *Appl. Optics* 49-1: 37-49 (2009)
[19] Knorsch, T., Heldmann, M., Hagedorn, T., Wensing, M., Leipertz, A., *16th Int. Symposia on Applications of Laser Techniques to Fluid Mechanics*, Lisbon, Portugal, July 9 - 12, 2012